Author Manuscript

Author Manuscript

Author Manuscript

Author Manuscript

HHS Public Access

Author manuscript

Circulation. Author manuscript; available in PMC 2021 February 11.

Published in final edited form as:

Circulation. 2020 February 11; 141(6): 464–478. doi:10.1161/CIRCULATIONAHA.119.042501.

Endothelial Cell-Derived IL-18 Released During Ischemia Reperfusion Injury Selectively Expands T Peripheral Helper Cells to Promote Alloantibody Production

Lufang Liu, MS[1,†], **Caodi Fang, MS**[1,†], **Whitney Fu, MD**[1,†], **Bo Jiang, MD**[2], **Guangxin Li, MD**[2], **Lingfeng Qin, MD**[2], **Jacob Rosenbluth**[3], **Gavin Gong, PhD**[3], **Catherine B. Xie, BS**[4], **Peter Yoo, MD**[2], **George Tellides, MD, PhD**[2], **Jordan S. Pober, MD, PhD**[4], **Dan Jane-wit, MD, PhD**[1,*]

[1]Division of Cardiovascular Medicine, Yale University School of Medicine, New Haven, CT 06520, USA;

[2]Dept of Surgery, Yale University School of Medicine, New Haven, CT 06520, USA;

[3]Collegiate School, New York, NY 10069;

[4]Dept of Immunobiology, Yale University School of Medicine, New Haven, CT 06520, USA

Abstract

Background-—Ischemia reperfusion injury (IRI) predisposes to formation of donor specific antibodies (DSA), a factor contributing to chronic rejection and late allograft loss.

Methods-—We describe a mechanism underlying the correlative association between IRI and DSA using humanized models and patient specimens.

Results-—IRI induces IgM-dependent complement activation on endothelial cells (ECs) which assembles an NLRP3 inflammasome via a Rab5-ZFYVE21-NIK axis and upregulates ICOS-L and PD-L2. EC-derived IL-18 selectively expands a T cell population (CD4+CD45RO+PD-1^{hi}ICOS+CCR2+CXCR5-) displaying features of recently described T peripheral helper (T_{PH}) cells. This population highly expressed IL-18R1 and promoted DSA in response to IL-18 *in vivo*. In patients with delayed graft function (DGF), a clinical manifestation of IRI, these cells were Ki-67+IL-18R1+ and could be expanded *ex vivo* in response to IL-18.

Conclusions-—IRI promotes elaboration of IL-18 from ECs to selectively expand alloreactive IL-18R1+ T_{PH} cells in allograft tissues to promote DSA formation.

Keywords

ischemia reperfusion injury; complement; membrane attack complexes; T peripheral helper cells; inflammasomes; IL-18; donor specific antibody

*Corresponding author: Dan Jane-wit, 10 Amistad St, room 437C, New Haven, CT 06519, Phone: 203-737-2869, dan.jane-wit@yale.edu., Fax: 203-737-2293.

†These authors contributed equally to the work.

CONFLICT OF INTEREST DISCLOSURES

All of the authors listed in this manuscript declare no financial conflicts of interest and have no financial disclosures.

Author Manuscript Author Manuscript Author Manuscript Author Manuscript

INTRODUCTION

Ischemia reperfusion injury (IRI) is a common complication of solid organ transplantation. In IRI, prolonged disruption of blood flow *ex vivo* leads to widespread tissue injury following surgical revascularization. Allografts with IRI show worsened survival and increased T cell- and antibody-mediated rejection episodes.[1] Vascular lesions often accompany and/or precede worsened clinical outcomes associated with IRI[2–4] and are correlated with anti-HLA alloantibodies, *de novo* donor specific antibody (dnDSA).[5] Vasculopathic changes are incorporated into the diagnostic criteria for chronic antibody-mediated rejection (CABMR), and in conjunction with dnDSA and vascular inflammation, reflect the consensus that most cases of graft failure >1 year post-transplantation are a result of immune-associated processes affecting the vasculature.[6–9]

Upon binding to graft class I or II HLA[3], both of which are highly expressed by human endothelial cells (ECs)[4], dnDSA may activate complement, a process associated with worsened outcomes compared to the presence of dnDSA alone.[10] Reduction of dnDSA[11] or blockade of complement is beneficial,[12] suggesting a causal relationship. Following transplantation, allograft ECs remain predominantly of donor origin[13] and thus persist as being targets for dnDSA. However, despite dnDSA and complement activation on these ECs, affected vascular beds in CABMR show preserved architectures without necrosis,[14] suggesting that complement may instead initiate inflammatory signaling. dnDSA-mediated complement activation resulting in endothelial MAC deposition elicits EC activation via a non-cytolytic, endosome-based process.[15–17] We have recently shown that endocytosed MAC triggers formation of an NLRP3 inflammasome and IL-1 secretion which is responsible for the observed autocrine/paracrine EC activation.[18] This process potentiates alloreactive CD4+ T activation.[18] Based on these data, we surmise that, in a manner linked to complement[19,20] and possibly inflammasome activation, processes linked to IRI could stimulate adaptive alloimmune responses[21,22] to elicit the chronic pathologies associated with CABMR.[23,24]

Tissue-derived B cells from CABMR patients express IgG and have thus undergone isotype switching. Moreover, B cell:T cell “conjugates” occur in graft tissues despite the absence of follicular DCs that present Ags to B cells within germinal centers[25] and despite the fact that T follicular helper cells (T_{FH} cells), the cells principally studied as promoting dnDSA,[26,27] canonically lack the battery of chemokine receptors required for vigorous peripheral tissue homing.[28,29] We developed humanized protocols of IRI where EC-mediated direct allorecognition occurs to study a response underlying these paradoxical observations. We report that human ECs subjected to IRI selectively activate a PD-1^{hi} CXCR5-CCR2+ memory T cell population to promote dnDSA and CABMR-like pathologies.

METHODS

Data Availability.

All data and methods are available from the authors upon reasonable request. The transciptomic datasets were retrieved from the Gene Expression Omnibus (accession #GSE50112) and Immport (accession #SDY939) public databases.

Author Manuscript Author Manuscript Author Manuscript Author Manuscript

Endothelial Cell Cultures.

All protocols were approved by the Yale Institutional Review Board. HUVEC were isolated as healthy, de-identified tissues from the Dept of Obstetrics and Gynecology at Yale New Haven Hospital as previously described.[1,2] IRI treatments are described in the Methods in the online-only Data Supplement.

Human CD4+ T Cell Isolation.

All protocols were approved by the Yale Institutional Review Board (Protocol #0601000969). PBMCs were isolated from leukopacks using density centrifugation as described previously and cryopreserved in liquid nitrogen.[13] CD4+CD45RO+ T cells were isolated from thawed cryovials using magnetic bead separation kits (Miltenyi) with HLA-DR Ab (clone L243, Novus #NB100–77855) and CD45RA Ab negative depletion (10μL per cryoival, eBiosciences, 14-0458-82).

Western Blot Analysis.

Western blots were performed as previously described.[13–15] Antibodies were used at 1:1000 at 4°C overnight as described in the Methods in the online-only Data Supplement.

Endothelial Cell:T Cell Cocultures.

For EC:T cell cocultures, HUVEC isolated from a single donor were grown in U-bottom 96-well microtiter plates, pretreated with human IFN-γ (50ng/mL, Invitrogen) for 48–72hr, and subjected to treatments as indicated in the text.

Animal Studies.

All protocols were approved by the Yale Institutional Animal Care and Use Committee and were performed in accordance with institutional guidelines. Human coronary arteries were interposed into the descending aortae of adult female C.B-17 SCID/beige mice (Taconic, Hudson, NY) for ~30 days to quiesce perioperative inflammation prior to use. Study details are described in Methods in the online-only Data Supplement.

DGF Patient Study.

All protocols were approved Yale Institutional Review Board (Protocol #2000020032), and participants gave informed consent. Study details are described in Methods in the online-only Data Supplement.

Immunofluorescence Analysis.

All protocols were approved Yale Institutional Review Board (Protocol #1212011221). Arterial tissues were flash frozen in OCT, sectioned, stained, and analyzed by I.F. as indicated.

Statistical Methods.

Comparisons between two groups were performed using two-sample *t*-test, and multiple comparisons were performed using a one-way or two-way ANOVA followed by Tukey's

Author Manuscript Author Manuscript Author Manuscript Author Manuscript

pairwise comparison test using Origin computer software. p-values <0.05 were considered statistically significant. Standard deviations are reported throughout the text.

RESULTS

Humanized Models of IRI to Recapitulate Features of CABMR.

To study connections between IRI and dnDSA, we adapted a humanized mouse model.[12,23] Paired human coronary artery segments are implanted as aortic interposition grafts in SCID/bg mice and subjected to anoxia or normoxia in organ culture prior to reparking into a second set of naïve SCID/bg hosts. Anoxic incubation conditions are necessary to mimic IRI because the artery segments are sufficiently thin walled to be well oxygenated by diffusion. As previously,[12] in "IRI"-treated xenografts we observed membrane attack complexes (MAC, PolyC9) in both ECs and smooth muscle cells (SMCs, Fig 1a). To study dnDSA formation, we retransplanted the normoxia- or "IRI"-treated human coronary artery segments into SCID/bg hosts engrafted with human PBMCs allogeneic to the artery donor. Circulating CD4+ (Fig S1a) and CD19+ (Fig S1b) lymphocytes increased with time but did not significantly differ between groups. CD4+:CD19+ ""conjugates"" were increased in hypoxia-treated arteries compared to controls (Fig S1c). The xenografts were harvested at four weeks post-implantation and analyzed. The intimal compartment was significantly increased in IRI-treated grafts compared to controls (Fig 1b). Neointimal tissue in IRI-treated grafts contained significantly higher CD4+ (Fig 1c) and CD19+ cells (Fig 1d), and contained CD4:CD19 "conjugates" (Fig 1e). No tertiary lymphoid organs were visualized in any host. To assess *de novo* donor specific antibody (dnDSA), sera were analyzed by clinical Luminex bead testing to determine antibody titers specific for the HLA haplotypes expressed on the implanted artery. Hosts bearing "IRI" grafts showed higher titers of dnDSA compared to controls (Fig 1f, left). Upon isotype analysis, dnDSA were enriched in IgG1 and IgG3, isotypes preferentially activating complement (Fig 1f, middle). To test dnDSA complement activation, we overlaid host sera on human ECs containing a matched HLA class I allele, HLA-B35. Sera from mice bearing IRI-treated grafts and higher titers of dnDSA were able to bind IgG and activate terminal complement (PolyC9) compared to ECs overlaid with control sera (Fig 1f, right). Human Abs in our model were produced at a composition of IgM>IgG>>IgA, IgD, and IgE (Fig 1g). Our humanized mouse model of IRI reproduced the diagnostic features of CABMR including complement-activating dnDSA.

"IRI" Elicits NLRP3 Inflammasome Assembly Via a Rab5-ZFYVE21-NIK Axis.

We developed an *in vitro* assay to define a mechanism linking IRI to dnDSA formation observed *in vivo*. We focused on ECs as these cells function as antigen presenting cells in humans, are principally affected by complement activation during IRI, and are sites where vasculopathic lesions form during CABMR. Pilot studies with cultured human ECs exposed to anoxic conditions followed by reoxygenation did not result in EC activation, but the conditions used did not consider complement activation, a key feature of CABMR, which was shown to be operative in our *in vivo* model of IRI (Fig 1a). In a revised model, ECs were pre-treated with IFN-γ to upregulate STAT1-dependent genes, a treatment enhancing inflammatory effects of complement,[15] and exposed to anoxia followed by normoxia in the presence of human serum to simulate ischemia and reperfusion, respectively. This treatment,

Author Manuscript Author Manuscript Author Manuscript Author Manuscript

which we call “IRI,” induced E-selectin (SELE) and CCL20 transcripts (Fig 1h) which were used as readouts in optimization studies with consideration to normoxia and hypoxia times (Fig S1d), cell confluency (Fig S1e), and buffer pH (Fig S1f). Following protocol optimization, we found that “IRI”, induced adhesion molecules (Fig 1i) and HIF1α, whose levels were not altered with IFN-γ or complement (Fig 1j). “IRI” furthermore elicited binding of IgM>>IgG (Fig 1k, left column) as well as early (C4d) and terminal (PolyC9) complement activation (Fig 1k, right column), consistent with findings in murine models of IRI.[31–33] To determine the relationship of IgM binding to complement activation, we subjected HUVEC to “IRI” in the presence of normal human sera containing wild-type (WT), factor B-deficient, or C1q-deficient sera. Compared to controls subjected to “IRI” with WT sera, MAC staining (PolyC9) was ablated in samples containing C1q-deficient (Fig 1l, left) but not factor B-deficient sera (Fig 1l, right), indicating that “IRI” required the classical or lectin pathway(s) for MAC assembly. We next examined the requirement for IgM for inducing MAC. We subjected HUVEC to “IRI” using total Ig-depleted human sera combined with exogenous IgM and/or IgG at concentrations approximating those of normal human sera. IgM (Fig 1m left) but not IgG (right) restored MAC in Ig-depleted cultures. In our prior model of alloAb-induced complement activation,[15] MAC initiated inflammatory signaling rather than invoking cytolysis of ECs. We found that, similar to these prior studies, EC viability was largely unaffected by “IRI” (Fig 1n). “IRI”-induced IgM-mediated MAC deposition on EC to elicit non-cytolytic EC activation.

We consequently phenotyped “IRI”-treated ECs, focusing on processes eliciting EC activation. IFN-γ transcriptionally upregulates inflammasome-related genes.[18] We consequently tested a role for IFN-γ in our “IRI” protocol. To do this we subjected EC to “IRI” with or without IFN-γ pretreatment and observed that “IRI” could induce transcriptional priming of caspase-1, IL1b, and IL18 in the absence of IFN-γ (Fig 2a) and that, following IFN-γ pretreatment, “IRI” did not further enhance levels of these genes (Fig 2b). On a protein level, expression of inflammasome components required reoxygenation and increased in proportion to the duration of post-anoxic normoxia (Fig 2c).

E-selectin and CCL20 were described as MAC-dependent genes upregulated by NIK,[15] however subsequent studies revealed these genes to be dependent on downstream NLRP3 inflammasomes, a process found to be NIK dependent.[18] We thus investigated whether “IRI” had induced inflammasome activation. Following priming, we observed inflammasome activation, characterized by phosphorylation of ASC (pASC), appearance of cleaved species of caspase-1 (~25kD), and presence of mature IL-18 in culture supernatants, during the normoxia phase of the protocol (Fig 2d). Treatment with caspase-1 inhibitors, Ac-YVAD-CMK and Ac-YVAD-FMK, decreased IL-18 (Fig 2e). As MAC were shown previously to utilize the NLRP3 sensor for inflammasome assembly,[18] we inhibited NLRP3 oligomerization with MCC950 and found that this treatment blocked IL-18 (Fig 2f). These data demonstrated that “IRI” primes and activates an NLRP3 inflammasome in EC to elicit IL-18 elaboration.

Rab5 is a small GTPase requiring various effector proteins to execute processes associated with subcellular trafficking. Rab5 effectors are defined operationally as binding to activated, i.e., GTP bound, Rab isoforms and as mediating downstream functions. We recently

Author Manuscript Author Manuscript Author Manuscript Author Manuscript

described ZFYVE21 as a Rab5 effector eliciting post-translational stabilization of NIK (NF-κB Inducing Kinase) on MAC+Rab5+ endosomes.[17] Following this process, endosome-associated NIK assembles an NLRP3 inflammasome.[18] We tested a requirement for this response in "IRI"-treated EC. With "IRI", we detected activated Rab5 (Rab5-GTP) and ZFVYE21 (Fig 2g) and EC stably transduced with Rab5 DN ablated induction of these molecules along with inflammasome activation, indicating a role for Rab5 activity with "IRI" (Fig 2h). ZFYVE21 siRNA blocked induction of NIK, resulting in decreased inflammasome activation and ablated IL-18 (Fig 2i). A Rab5-ZFYVE21-NIK axis was required for inflammasome assembly in ECs following "IRI."

We next provisionally assessed HLA and costimulatory molecules in "IRI"-treated EC. We observed that "IRI" had no effect on HLA expression but rather upregulated ICOS-L and PD-L2 and to a lesser extent, LFA-3 and PD-L1 (Fig 2j). We examined the role of inflammasome-derived cytokines on expression of these molecules and found that dual but not individual neutralization of IL1β and IL18 prevented "IRI" induction of ICOS-L but had no effect on PD-L2 (Fig 2k). Together, our data indicated that "IRI" could elicit EC activation in an inflammasome-dependent manner.

IRI-Treated EC Selectively Expand Functional T_{PH} Cells *In Vitro*.

The development of IgG+ dnDSA in our *in vivo* model of IRI (Fig 1f) suggested that alloreactive B cells had undergone isotype switching, a process requiring CD4+ T cell help. Initially, we assessed interactions of "IRI"-treated EC with allogeneic CD4+CD45RO+ memory T cells (T_{mem}) using EC:T cell cocultures. In this system, human EC function as antigen presenting cells to elicit T cell responses via direct allorecognition, a response we surmised may have occurred *in vivo* (Fig 1c). "IRI"-treated ECs enhanced T_{mem} activation as assessed by expression of HLA-DR (Fig 3a, top), an activation marker, and by dilution of carboxyfluorescein diacetate succinimidyl ester, a marker of cell proliferation (CFSE, Fig 3a, bottom). To assess a requirement for complement in this process, we subjected ECs to "IRI" in the presence of C1q-deficient or C6-deficient human reference sera lacking the ability to activate the classical pathway or to assemble MAC, respectively. The enhanced T cell activation observed in "IRI" cocultures was significantly reduced in cultures containing C1q- or C6-deficient sera (Fig 3b), indicating that MAC assembly resulting from the classical pathway was required for "IRI"-treated EC to enhance T_{mem} activation.

We subsequently sought to identify subset(s) within the T_{mem} population activated by "IRI"-treated ECs. We initially focused on T follicular (T_{FH}) helper T_{PH} cells, which are a T cell subset expressing ICOS, PD-1, and CXCR5 with specialized ability to provide T cell help in Ab responses. Upon further gating of T_{mem}, we observed three populations of HLA-DR+ T cells based on PD-1^{lo}, PD-1^{mid}, or PD-1^{hi} expression. Contrary to our initial hypothesis we consistently detected higher frequencies of HLA-DR+ cells within the ICOS +PD-1^{hi}CXCR5- population *vs* ICOS+PD1^{hi}CXCR5+ T cells whose surface phenotype is consistent with circulating T_{FH} cells (Fig 3c, top row). We speculated that the expanded T cell population lacking CXCR5 expression might belong to a recently described CD4+ T cell subset designated as T peripheral helper (T_{PH}) cells[25] which, like T_{FH} cells, express ICOS and PD-1, cognate ligands, ICOS-L and PD-L2, upregulated by "IRI" in EC (Fig 2j)

Author Manuscript Author Manuscript Author Manuscript Author Manuscript

but in contrast show decreased bcl-6 to BLIMP1 ratios[28,34] and express chemokine receptors allowing migration to tissues including CCR2, CX3CR1, and CCR5.[28] CXCR5, in contrast, binds to a single ligand, CXCL13, which is discretely expressed in the follicular mantle zone of secondary lymphoid organs to putatively confer differential homing.[26–29] Further analyses revealed that the CXCR5- population significantly expressed higher levels of ICOS and were enriched in CCR2 (Fig 3c, middle row), prompting use of this marker in downstream analyses. HLA-DR+PD-1^{hi}CXCR5-CCR2+ T_{mem} were selectively expanded by "IRI"-treated ECs when compared to HLA-DR+PD-1^{hi}CXCR5+CCR2+ T_{mem} (Fig 3c, bottom). PD-1^{hi}ICOS+CCR2+ T_{mem} in healthy donors were observed at low frequencies, but when placed in EC:T cell cocultures after FACS-sorting, were also selectively expanded by "IRI"-treated EC when compared to circulating T_{FH} cells (Fig 3d, right). Although percent recovery of PD-1^{hi}CCR2-CXCR5+ T_{mem} from healthy donors was lower than PD-1^{hi}CCR2+CXCR5- T_{mem}, these differences were not significant (Fig 3d, left).

We phenotyped the "IRI"-expanded T cell population gated above to test whether this population behaved like described T_{PH} cells. Consistent with the published phenotype,[25] the gated cells above showed low ratios of bcl-6:BLIMP1 (Fig 3e) that were not substantially altered by coculture with "IRI"-treated EC, and expressed IFN-γ- and IL-21 but not IL-4, (Fig 3f), recapitulating a type 1 effector profile seen in T_{FH} cells.[31,32] When EC were subjected to "IRI" and cocultured with these gated cells or T_{FH} cells along with autologous CD220+ B cells, cultures containing the gated cells showed increased dnDSA titers specific for the HLA expressed on the cultured EC (Fig 3g). dnDSA consisted primarily of anti-HLA class I Ab and to a much lesser degree anti-HLA class II Ab. The dnDSA produced were mostly comprised of IgG1 Abs (Fig 3h). Similar to our *in vivo* model, alloAbs consisted of IgM>IgG>>IgA, IgD, and IgE (Fig 3i). Our gated population were PD-1^{hi}, ICOS+, and CCR2+; showed low bcl6:BLIMP1 ratios; elaborated IL-21; and elicited Ab production from B cells. Taken together, the surface, transcriptional, and functional phenotype of the T cell population expanded in "IRI" EC:T cell and EC:T cell:B cell cocultures were consistent with that of T_{PH} cells. Based on this we concluded that "IRI"-treated EC preferentially activated T_{PH} cells with a type 1 effector phenotype that were capable of eliciting dnDSA from alloimmune B cells.

IL-18 Directly Expands IL-18R1+ T_{PH} Cells.

Based on the observation that "IRI" induced both inflammasome activation (Fig 2) and T_{PH} cell expansion (Fig 3), we examined the effects of IL-18 on T_{PH} cells. We found that caspase-1 inhibition abrogated the ability of "IRI"-treated EC to activate T_{PH} cells and that this inhibition was relieved by addition of IL-18 (Fig 4a). A similar effect was observed with MCC950, an NLRP3 inhibitor, whose effects could be derepressed with exogenous IL-18 (Fig 4b). We found that αIL-18 Ab, when added to "IRI" cocultures containing T_{mem}, reduced frequencies of activated T_{PH} cells (Fig 4c, left) while exogenous IL-18 potentiated activated T_{PH} cells (Fig 4c, right). bcl-6:BLIMP1 ratios among activated T_{mem} in "IRI" cocultures were significantly reduced compared to controls and were significantly increased with αIL-18 Ab. In contrast, bcl6:BLIMP1 ratios were reduced in control cocultures with IL-18 (Fig 4d, right). As "IRI" cocultures did not significantly alter bcl-6:BLIMP1 ratios among T_{PH} cells or T_{FH} cells (Fig 3e), we interpreted these results as meaning that IL-18

Author Manuscript Author Manuscript Author Manuscript Author Manuscript

had lowered bcl-6:BLIMP1 ratios in T_{mem} due to preferential expansion of T_{PH} cells *vs* T_{FH} cells and not to potentiated reduction of bcl-6:BLIMP1 ratios among existing T_{PH} cells.

Given the effects of IL-18 above, we analyzed public transcriptomic datasets[25] and found higher IL18R1 reads by RNA seq in HLA-DR+ICOS+CXCR5- T cells *vs* HLA-DR+ICOS +CXCR5+ T cells. We thus interrogated expression of IL-18R1 on T_{PH} cells. "IRI"-treated ECs significantly increased IL-18R1+ T cells within T_{mem} (Fig 4e). Upon gating on T_{PH} or T_{FH} cells, we observed a significant enrichment of IL-18R1 on T_{PH} cells *vs* T_{FH} cells (Fig 4f). Upon reciprocal gating on T_{PH} and T_{FH} cells, we observed that percentages of activated IL-18R1+ T cells was significantly higher in T_{PH} cells *vs* T_{FH} cells (Fig 4g). To discern whether IL-18 acted directly upon "IRI"-treated EC and/or T_{PH} cells, we activated FACS-sorted T_{PH} or T_{FH} cells with αCD3/CD28 in the absence of EC and with IL-18 and observed significant expansion of T_{PH} cells but not T_{FH} cells (Fig 4h). The expanded T_{PH} cells highly expressed IL-18R1, indicating a direct role of IL18 on IL-18R1+ T_{PH} cells but not T_{FH} cells (Fig 4i). To confirm our findings, we knocked down IL-18R1 on EC and/or T_{mem} using gene-specific shRNA. In pilot studies, we found that IL18R1 expression was enhanced by "IRI" in both EC (Ulex) and T_{PH} cells (Fig 4j, left). In contrast to IL-18R1 knockdowns on EC, IL-18R1 knockdowns on T_{mem} significantly abrogated "IRI"-induced expansion of T_{PH} cells, an effect that was reduced to levels below normoxia controls in cultures containing knockdowns of IL-18R1 in both EC and T_{mem} (Fig 4j, right). These data indicated that IL-18 directly expanded IL-18R1+ T_{PH} cells.

IRI-Induced Inflammasomes in EC and IL-18-Mediated T_{PH} Cell Expansion *In Vivo*.

In light of our findings, we expanded our analysis of IRI-treated artery segments to identify IRI-induced differences relevant for T_{PH} cell activation *in vivo*. IRI treatment assembled an inflammasome *in vivo* in both ECs and smooth muscle cells (αSMA) as detected by increased intimal and medial FLICA (Fluorescent Inhibitor of Caspase Activation) staining, a fluorogenic readout for cleaved caspase-1 (Fig 5a). We also detected increased human IL-18 in sera from "IRI"-treated hosts compared to controls (Fig 5b,c). IRI-treated grafts showed linear staining of ICOS-L and PD-L2 on ECs but not in smooth muscle cells, where staining for these molecules appeared punctate, consistent with their expression on immune cells (Fig 5d). Analysis of circulating human lymphocytes revealed increased T_{PH} cells but not T_{FH} cells (Fig S2a) expressing IFN-γ and IL-21 but not IL-4 (Fig S2b). IL-18R1 expression was significantly increased in hosts bearing IRI-treated grafts among T_{PH} cells (Fig S2c). Further analysis of tissue-infiltrating CD4+ T cells showed significantly increased numbers of T_{PH} cells but not T_{FH} in the neointima of IRI-treated grafts (Fig 5e). These data, corroborating our *in vitro* findings, demonstrated that IRI induced inflammasome activation and T_{PH} cell recruitment to activated ECs *in vivo*.

We next interrogated a role for IL-18 in the *in vivo* expansion of T_{PH} by supplementing hosts bearing normoxia-treated human artery segments and allogeneic PBMCs with exogenous PBS or IL-18. Treatment with human IL-18 increased circulating T_{PH} cells but not T_{FH} cells (Fig S3a) as well as percentages of circulating plasmablasts (Fig S3b). Morphometric analyses showed that IL-18-treated grafts showed significantly increased neointimal area and reduced luminal areas (Fig 5f). Compared to PBS-treated hosts, IL-18-

Author Manuscript Author Manuscript Author Manuscript Author Manuscript

treated tissues showed increased neointimal T_{PH} cells > T_{FH} cells (Fig 5g), and neointimal CD19+CD27+ B cells (Fig 5h). We also detected neointimal CD4+:CD19+ ""conjugates"" (Fig 5i). Anti-HLA Ab testing revealed increased dnDSA titers in IL-18-treated hosts (Fig 5j, left) and that IgG isotype titers consisted predominantly of IgG1 and IgG3 (Fig 5j, right) with an Ab composition of IgM>IgG>>IgA, IgD, and IgE (Fig 5k). These data showed that IRI could promote dnDSA formation through the actions of EC-derived IL-18 on alloreactive T_{PH} cells.

Splenic B cells generate dnDSA in murine models,[26,27] and tissue-infiltrating B cells, though highly correlative with allograft outcomes in patients,[35,36] when isolated and expanded, produce Igs broadly reactive with altered self-antigens rather than dnDSA.[37] At the time of dnDSA generation, we quantified follicles in splenic tissues. Compared to normal human tonsillar tissue as controls (Fig S3c, left), the total number of follicles were very low among all host groups (Fig S3c, right), and no secondary follicles were observed. IL-18, known to induce lymphoid hyperplasia, induced a small but significant increase in follicles (Fig S3c), but these numbers poorly correlated with IgG levels (Fig S3d, r=0.06, left) which instead showed much higher correlations with the number of neointimal T_{PH} cells (Fig S3d, r=0.62, right). The lack of splenic follicles in our humanized model, likely due to a lack of human myeloid cells and/or follicular DCs, suggested that the bulk of observed dnDSA were generated by graft-infiltrating B cells.

IL-18-Dependent Expansion of IL-18R1+ T_{PH} Cells in DGF Patients.

We analyzed archived renal biopsies of DGF patients with CABMR by I.F., and we prospectively analyzed sera and PBMCs from DGF (n=8) and control renal transplant patients (n=10). Compared to controls, biopsies with CABMR showed staining for VCAM-1 colocalizing with EC in peritubular capillaries (PTC, Fig 6a). PTC also showed staining for cleaved caspase-1 (Fig 6b) indicating inflammasome activation in EC. EC also showed ICOS-L and PD-L2 expression within glomeruli (Fig 6c). CABMR tissue contained significantly higher infiltrates of glomerular T_{PH} cells when compared to T_{FH} cells (Fig 6d). We further detected T cell:B cell:EC "conjugates" (Fig 6e).

We then analyzed sera and PBMCs from DGF patients and controls. Baseline patient data showed significantly higher titers of panel reactive antibody (PRA) and longer hospitalizations in DGF patients *vs* controls, while other clinical parameters were not significantly different (Table 1). In patient sera, we detected significantly increased circulating Sc5b-9 (Fig 6f), a marker of terminal complement activation, in DGF patients whom additionally showed higher serum IL-18, although this analysis did not reach statistical significance (Fig 6g) This finding contrasts with urinary IL-18, whose levels strongly correlate with DGF.[38,39] These data supported our biopsy staining results and indicated that complement and inflammasome activation had occurred in association with clinical IRI.

Cytometry by time-of-flight (CyTOF) or mass cytometry uses rare metal- rather than fluorophore-tagged Abs to allow multiparameter analyses using low input cell numbers. Analogous to our *in vitro* findings, mass cytometry of patient PBMCs showed that DGF patients contained an expanded population of T_{mem} with high expression of PD-1 and ICOS

Author Manuscript Author Manuscript Author Manuscript Author Manuscript

(Fig 6h, left). Upon gating on these cells, we observed increased percentages of T_{PH} cells but not circulating T_{FH} cells (Fig 6h, right). Further phenotyping of the expanded T_{PH} cell population showed that these cells were enriched within the effector memory T cell population (CD4+CD45RO+CCR7-), suggesting that T_{PH} cells had acquired an increased capability for tissue homing (Fig 6i). In DGF patients a significantly higher percentage of T_{PH} cells produced IFN-γ but not IL-4 or IL-21 upon *ex vivo* stimulation (Fig 6j).

We next assessed IL-18-IL-18R1 interactions in the expanded T_{PH} cell population. IL-18R1 was highly expressed among T_{mem} in DGF patients *vs* controls (Fig 6k, left) and this enrichment was driven by IL-18R1 expression on T_{PH} cells (Fig 6k, right). The percentage of T_{PH} cells expressing IL-18R1 was increased upon *ex vivo* stimulation (Fig 6l), in alignment with our *in vitro* results (Fig 4e–g). Moreover, DGF patients showed increased Ki-67 expression among T_{PH} cells, and this effect was remarkably lost upon further gating on IL-18R1- T_{PH} cells but not IL-18R1+ T_{PH} cells (Fig 6m) indicating that IL-18R1+ T_{PH} cells had selectively undergone proliferation in DGF patients endogenously. To test the functional significance of IL-18 on T_{PH} cells, we added sera from DGF or control patients to non-autologous T_{mem} stimulated with αCD3/CD28 with or without αIL-18 Ab (Fig 6n) or exogenous IL-18 (Fig 6o). Upon stimulation, we found that the percentages of activated T_{PH} cells were significantly increased in cultures containing DGF sera *vs* control sera (Fig 6n, lane 4 *vs* lane 6). This potentiated expansion of T_{PH} cells in cultures containing DGF sera was abrogated by αIL-18 Ab (Fig 6n, lane 6 *vs* lane 7 and lane 8 *vs* lane 9). Conversely, IL-18, when added to T_{mem} cultures containing DGF sera significantly boosted T_{PH} cell percentages (Fig 6o, lane 8 *vs* lane 9). We observed that samples containing DGF sera showed reduced T_{PH} cell percentages compared to samples without sera (Fig 6n–o, lane 1 *vs* lane 6 and lane 1 *vs* lane 8), likely due to the presence of immunosuppressives in patient sera. Data derived from clinical samples, a portion of which were collected prospectively, aligned with our *in vitro* and *in vivo* findings and showed that IL-18 released in association with IRI could expand T_{PH} cells enriched in IL-18R1.

DISCUSSION

We describe a mechanism linking IRI-induced complement activation on EC with the development of dnDSA (Fig 6p) which may occur at the tissue level to alter and/or augment splenic-derived alloimmune responses. Under conditions of high antigen load, conventional dendritic cells are dispensable for the generation of T_{FH} cells which show significantly impaired but not ablated ability to elicit Ab responses.[40,41] These data imply alternative source(s) of antigen presentation, presumably B cells,[40] but could include ECs to elicit Ab responses. Our humanized models permitting direct allorecognition mimics such a process where Ab responses are detectable despite the absence of significant T_{FH} cell responses and demonstrate that B cell maturation can occur within peripheral tissues.

For such a response to occur, direct allorecognition between HLA class I or II molecule(s) on activated EC with both an alloimmune T_{PH} cell and B cell precedes contact- or cytokine-dependent interactions between the same T_{PH} cell and B cell to allow for full B cell maturation. In this paradigm, activated ECs and T_{PH} cells function analogously to follicular DCs and T_{FH} cells and as such, analogous step(s) in T_{FH} cell generation (reviewed in ref

Author Manuscript Author Manuscript Author Manuscript Author Manuscript

42), e.g., sequential activation of transcription factors and spatial cues, may apply for T_{PH} cell development. T_{mem} expressing ICOS+PD-1hiCXCR5- are expanded in autoimmune conditions including RA,[25,43] SLE,[44] and celiac disease.[45] Our human data similarly show expansion of such a population in DGF patients which is contained within the effector memory population and may respond to EC-derived signals that putatively specify maturation information as above.

Our "IRI" studies implicate natural IgM Abs similar to prior reports.[31–33] The preponderance of IgM in both our *in vitro* and *in vivo* models suggests that though IRI-activated ECs potentiate dnDSA responses, graft-infiltrating B cells may not undergo efficient class switching in peripheral tissues *vs* secondary lymphoid organs as suggested by Zorn and colleagues,[37] though this remains to be tested and could instead reflect an artifactual feature of our humanized mouse model that, similar to other humanized models,[46] may not fully support robust isotype switching. Moreover, the pathological potential of dnDSA observed in our models, though shown to be complement-activating, is unknown and at this juncture remains a correlative rather than causative finding for CABMR. Clinical Luminex testing used herein reports MFIs of total IgG binding to HLA class I and II and does not convey information regarding IgG subtypes, anti-HLA IgM, or non-HLA binding anti-endothelial alloAbs. IgG+ dnDSA MFIs were measured in Fig 1f, 3g, and 5j, whereas total IgM and IgG titers in ng/mL were assessed in Fig 1g, 3i, 5k. In these latter studies, bulk Ab quantities did not distinguish between dnDSA, polyreactive Ab, or a mixture of the above and in clinical settings is of limited prognostic value and merely reflected a proof of principle of increased T_{PH} helper cell functionality with IRI or IL-18. With these caveats, future studies characterizing these alloAbs will increase clinical relevance of our work.

Supplementary Material

Refer to Web version on PubMed Central for supplementary material.

ACKNOWLEDGMENTS

L.L., C.F., W.F., and D.J. performed all of the experiments. L.Q., B.J., G.L., and G.T. participated in experiments involving surgical procedures. J.R. and G.G. analyzed biopsy samples. C.F., J.S.P., and D.J. analyzed and interpreted experimental results. W.F., C.F., S.G., and R.T. were involved in patient sample collection, archiving, and processing. D.J. designed all of the experiments. D.J. drafted the manuscript.

FUNDING SOURCES

J.S.P. was supported by grants from the NIH (R01HL-51014). D.J. was supported by grants from the NIH (R01HL141137-01, R00HL125895, UL1TR001863) and Vasculitis Foundation (P30AR053495-01A1).

Non-standard Abbreviations and Acronyms:

Ag	antigen
C'	complement
CABMR	chronic antibody-mediated rejection
CFSE	carboxyfluorescein diacetate succinimidyl ester

Author Manuscript Author Manuscript Author Manuscript Author Manuscript

CyTOF	cytometry by time-of-flight
dnDSA	*de novo* donor specific antibody
Follicular DCs	follicular dendritic cells
HUVECs	human umbilical vein endothelial cells
IRI	ischemia reperfusion injury
MAC	membrane attack complexes
PRA	panel reactive antibody
T_{FH} cell	T follicular helper cell
T_{PH} cell	T peripheral helper cell

REFERENCES

1. Wu WK, Famure O, Li Y, Kim SJ. Delayed graft function and the risk of acute rejection in the modern era of kidney transplantation. Kidney Int. 2015;88:851–858. [PubMed: 26108067]
2. Levine DJ, Glanville AR, Aboyoun C, Belperio J, Benden C, Berry GJ, Hachem R, Hayes D Jr, Neil D, Reinsmoen NL, et al. Antibody-mediated rejection of the lung: a consensus report of the International Society for Heart and Lung Transplantation. J Heart Lung Transplant. 2016; 35:397–406. [PubMed: 27044531]
3. Demetris AJ, Bellamy C, Hubscher SG, O'Leary J, Randhawa PS, Feng S, Neil D, Colvin RB, McCaughan G, Fung JJ, et al. Comprehensive update of the Banff Working Group on Liver Allograft Pathology: introduction of antibody-mediated rejection. Am J Transplant. 2016;16:2816–2835. [PubMed: 27273869]
4. Haas M, Loupy A, Lefaucheur C, Roufosse C, Glotz D, Seron D, Nankivell BJ, Halloran PF, Colvin RB, Akalin E, et al. The Banff 2017 Kidney Meeting Report: revised diagnostic criteria for chronic active T cell-mediated rejection, antibody-mediated rejection, and prospects for integrative endpoints for next-generation clinical trials. Am J Transplant. 2018;18:293–307. [PubMed: 29243394]
5. Wiebe C, Gibson IW, Blydt-Hansen TD, Karpinski M, Ho J, Storsley LJ, Goldberg A, Birk PE, Rush DN, Nickerson PW. Evolution and clinical pathologic correlations of de novo donor-specific HLA antibody post kidney transplant. Am J Transplant. 2012;12:1157–1167. [PubMed: 22429309]
6. Loupy A, Lefaucheur C. Antibody-Mediated Rejection of Solid-Organ Allografts. N Engl J Med. 2018;379:1150–1160. [PubMed: 30231232]
7. Bruneval P, Angelini A, Miller D, Loupy A, Zeevi A, Reef EF, Dragun D, Reinsmoen N, Smith RN, West L, et al. The XIIIth Banff Conference on Allograft Pathology: the Banff 2015 heart meeting report: improving antibody-mediated rejection diagnostics: strengths, unmet needs, and future directions. Am J Transplant. 2017;17:42–53. [PubMed: 27862968]
8. Wallace WD, Li N, Andersen CB, Arrossi AV, Askar M, Berry GJ, DeNicola MM, Neil DA, Pavlisko EN, Reed EF, et al. Banff study of pathologic changes in lung allograft biopsy specimens with donor-specific antibodies. J Heart Lung Transplant. 2016;35:40–48. [PubMed: 26601715]
9. O'Leary JG, Michelle Shiller S, Bellamy C, Nalesnik MA, Kaneku H, Jennings LW, Isse K, Terasaki PI, Klintmalm GB, Demetris AJ, et al. Acute liver allograft antibody-mediated rejection: an inter-institutional study of significant histopathological features. Liver Transpl. 2014;20:1244–1255. [PubMed: 25045154]
10. Loupy A, Lefaucheur C, Vernerey D, Pregger C, Duong van Hueyn JP, Mooney N, Suberbielle C, Fremeaux-Bacchi V, Mejean A, Desgrandchamps F, et al. Complement-binding anti-HLA antibodies and kidney-allograft survival. N Engl J Med. 2013;369:1215–1226. [PubMed: 24066742]

Author Manuscript Author Manuscript Author Manuscript Author Manuscript

11. Everly MJ, Everly JJ Arend LJ, Brailey P, Susskind B, Govil A, Rike A, Roy-Chaudhury P, Mogilishetty G, Alloway RR, et al. Reducing de novo donor-specific antibody levels during acute rejection diminishes renal allograft loss. Am J Transplant. 2009;9:1063–1071. [PubMed: 19344434]
12. Qin L, Li G, Kirkiles-Smith N, Clark P, Fang C, Wang Y, Yu ZX, Devore D, Tellides G, Pober JS, Jane-wit D. Complement C5 Inhibition Reduces T Cell-Mediated Allograft Vasculopathy Caused by Both Alloantibody and Ischemia Reperfusion Injury in Humanized Mice. Am J Transplant. 2016;16:2865–2876. [PubMed: 27104811]
13. Lagaaij EL, Cramer-Knijnenburg GF, van Kemenade FJ, van Es LA, Bruijn JA, van Krieken JH. Endothelial cell chimerism after renal transplantation and vascular rejection. Lancet. 2001;357:33–37 [PubMed: 11197359]
14. Valenzuela NM, Reed EF. Antibody-mediated rejection across solid organ transplants: manifestations, mechanisms, and therapies. J Clin Invest. 2017; 127:2492–2504. [PubMed: 28604384]
15. Jane-Wit D, Manes TD, Yi T, Qin L, Clark P, Kirikiles-Smith NC, Abrahimi P, Devalliere J, Moeckel G, Kulkarni S, Tellides G, Pober JS. Alloantibody and complement promote T cell-mediated cardiac allograft vasculopathy through noncanonical nuclear factor-kappaB signaling in endothelial cells. Circulation. 2013;128:2504–2516. [PubMed: 24045046]
16. Jane-wit D, Surovtseva YV, Qin L, Li G, Liu R, Clark P, Manes TD, Wang C, Kashgarian M, Kirkiles-Smith NC, Tellides G, Pober JS. Complement membrane attack complexes activate noncanonical NF kappaB by forming an Akt+ NIK+ signalosome on Rab5+ endosomes. Proc Natl Acad Sci U S A. 2015;112:9686–9691. [PubMed: 26195760]
17. Fang C, Manes TD, Liu L, Liu K, Qin L, Li G, Tobiasova Z, Patel M, Merola J, Fu W, Liu R, Xie C, Tietjen GT, Nigrovic PA, Tellides G, Pober JS, Jane-wit D. ZFYVE21 is a Complement-Induced Rab5 Effector That Activates Non-Canonical NF-kB Via Phosphoinosotide Remodeling of Endosomes. Nat Commun. 2019;10: 2247. [PubMed: 31113953]
18. Xie CB, Qin L, Li G, Fang C, Kirkiles-Smith NC, Tellides G, Pober JS, Jane-wit D. Internalized Complement Membrane Attack Complexes Assemble NLRP3 Inflammasomes Triggering Autocrine IL-1 Activation of IFN-γ-Primed Human Endothelium. Circ Res. 2019 124:1747–1759. [PubMed: 31170059]
19. Gorsuch WB, Chrysanthou E, Schwaeble W, Stahl GL. The Complement System in Ischemia-Reperfusion Injuries. Immunobiology. 2012;217:1026–1033. [PubMed: 22964228]
20. Halloran PF, Homik J, Goes N, Lui SL, Urmson J, Ramassar V, Cockfield SM. The “injury response”: a concept linking nonspecific injury, acute rejection, and long-term transplant outcomes. Transplant Proc. 1997;29:79–81. [PubMed: 9123164]
21. Fuquay R, Renner B, Kulik L, McCullough JW, Amura C, Strassheim D, Pelanda R, Torres R, Thurman JM. Renal ischemia-reperfusion injury amplifies the humoral immune response. J Am Soc Nephrol. 2013;24:1063–1072. [PubMed: 23641055]
22. Yi T, Fogal B, Hao Z, Tobiasova Z, Wang C, Rao DA, Al-Lamki RS, Kirkiles-Smith NC, Kulkarni S, Bradley JR, et al. Reperfusion injury intensifies the adaptive human T cell alloresponse in a human-mouse chimeric artery model. Arterioscler Thromb Vasc Biol. 2012;32:353–60. [PubMed: 22053072]
23. Pober JS, Jane-wit D, Qin L, Tellides G. Interacting mechanisms in the pathogenesis of cardiac allograft vasculopathy. Arterioscler Thromb Vasc Biol. 2014;34:1609–1614. [PubMed: 24903097]
24. Cioni M, Nocera A, Innocente A, Tagliamacco A, Trivelli A, Basso S, Quartuccio G, Fontana I, Magnasco A, Drago F, et al. De Novo Donor-Specific HLA Antibodies Developing Early or Late after Transplant Are Associated with the Same Risk of Graft Damage and Loss in Nonsensitized Kidney Recipients. J Immunol Res. 2017;1747030. [PubMed: 28367453]
25. Rao DA, Gurish MF, Marshall JL, Shlowikowski K, Fonseka CY, Liu Y, Donlin LT, Henderson LA, Wei K, Mizoguchi F, et al. Pathologically expanded peripheral T helper cell subset drives B cells in rheumatoid arthritis. Nature. 2017;542:110–114. [PubMed: 28150777]
26. Walters GD, Vinuesa CG. T Follicular Helper Cells in Transplantation. Transplantation. 2016;100:1650–1655. [PubMed: 27362303]

Author Manuscript Author Manuscript Author Manuscript Author Manuscript

27. Badell IR, Ford ML. T follicular helper cells in the generation of alloantibody and graft rejection. Curr Opin Organ Transplant. 2016;21:1–6. [PubMed: 26727455]

28. Crotty S A brief history of T cell help to B cells. Nat Rev Immunol. 2015;15:185–189. [PubMed: 25677493]

29. Alsughayyir J, Pettigrew GJ, Motallebzadeh R. Spoiling for a Fight: B Lymphocytes As Initiator and Effector Populations within Tertiary Lymphoid Organs in Autoimmunity and Transplantation. Front Immunol. 2017;8:1639. [PubMed: 29218052]

30. Pober JS, Jane-wit D, Qin L, Tellides G. Interacting mechanisms in the pathogenesis of cardiac allograft vasculopathy. Arterioscler Thromb Vasc Biol. 2014;34:1609–1614. [PubMed: 24903097]

31. Marshall K, Jin J, Atkinson C, Alawieh A, Qiao F, Lei B, Chavin KD, He S, Tomlin S. Natural immunoglobulin M initiates an inflammatory response important for both hepatic ischemia reperfusion injury and regeneration in mice. Hepatology. 2017;67:721–735. [PubMed: 28880403]

32. Kulik L, Fleming SD, Moratz C, Reuter JW, Novikov A, Chen K, Anderews KA, Markaryan A, Quigg RJ, Silverman GJ, et al. Pathogenic natural antibodies recognizing annexin IV are required to develop intestinal ischemia-reperfusion injury. J Immunol. 2009;182:5363–5373. [PubMed: 19380783]

33. van der Pol P, Roos A, Berger SP, Daha MR, van Kooten C. Natural IgM antibodies are involved in the activation of complement by hypoxic human tubular cells. Am J Renal Physiol. 2011;300:F932–F940.

34. Johnston RJ , Poholek AC, DiToro D, Yusuf I, Eto D, Barnett B, Dent AL, Craft J, Crotty S. Bcl-6 and Blimp-1 are reciprocal and antagonistic regulators of T follicular helper cell differentiation. Science. 2009;325:1006–1010. [PubMed: 19608860]

35. Chang A, Moore JM, Cowan ML, Josephson MA, Chon WJ, Sciammas R, Du Z, Marino SR, Meehan SM, Millis M, et al. Plasma cell densities and glomerular filtration rates predict renal allograft outcomes following acute rejection. Transpl Int. 2012;25:1050–1058. [PubMed: 22805456]

36. Lu Y, Li B, Shen Q, Wang R, Chen Z, Jiang H, Chen J. Effects of CD20+ B-cell infiltration into allografts on kidney transplantation outcomes: a systematic review and meta-analysis. Oncotarget. 2017;8:37935–37941. [PubMed: 28415773]

37. Ferdman J, Porcheray F, Gao B, Moore C, DeVito J, Dougherty S, Thomas MV, Farkash EA, Elias N, Kawai T, et al. Expansion and somatic hypermutation of B-cell clones in rejected human kidney grafts. Transplantation. 2014;98:766–772. [PubMed: 24825521]

38. Parikh CR, Jani A, Mishra J, Ma Q, Kelly C, Barasch J, Edelstein CL, Devarajan P. Urine NGAL and IL-18 are predictive biomarkers for delayed graft function following kidney transplantation. Am J Transplant. 2006;6:1639–1645. [PubMed: 16827865]

39. Lee EY, Kim MS, Park Y, Kim HS. Serum neutrophil gelatinase-associated lipocalin and interleukin-18 as predictive biomarkers for delayed graft function after kidney transplantation. J Clin Lab Anal. 2012;26:295–301. [PubMed: 22811364]

40. Barnett LG, Simkins HM, Barnett BE, Korn LL, Johnson AL, Wherry EJ, Wu GF, Laufer TM. B cell antigen presentation in the initiation of follicular helper T cell and germinal center differentiation. J Immunol. 2014;192:3607–3617. [PubMed: 24646739]

41. Dahlgran MW, Gustafsson-Hedberg T, Livingston M, Cucak H, Alsén S, Yrlid U, Johansson-Lindbom B. T follicular helper, but not Th1, cell differentiation in the absence of conventional dendritic cells. J Immunol. 2015;194:5187–5199. [PubMed: 25917099]

42. Linterman MA, Vinuesa CG. Signals that drive T follicular helper cell formation. Immunology. 2017;152:185–194. [PubMed: 28628194]

43. Fortea-Gordo P, Nuño L, Villalba A, Peiteado D, Monjo I, Sánchez-Mateos P, Puig-Kröger A, Balsa A, Miranda-Carús ME. Two populations of circulating PD-1hiCD4 T cells with distinct B cell helping capacity are elevated in early rheumatoid arthritis. Rheumatology. 2019; 58:1662–1673. [PubMed: 31056653]

44. Lin J, Yu Y, Ma J, Ren C, Chen W. PD-1+CXCR5-CD4+T cells are correlated with the severity of systemic lupus erythematosus. Rheumatology. 2019. doi: 10.1093/rheumatology/kez228.

45. Christophersen A, Lund EG, Snir O, Solà E, Kanduri C, Dahal-Koirala S, Zühlke S, Molberg Ø, Utz PJ, Rohani-Pichavant M, Simard JF, Dekker CL, Lundin KEA, Sollid LM, Davis MM.Distinct

Author Manuscript Author Manuscript Author Manuscript Author Manuscript

phenotype of CD4+ T cells driving celiac disease identified in multiple autoimmune conditions. Nat Med. 2019;25:734–737. [PubMed: 30911136]

46. Yu H, Borsotti C, Schickel JN, Zhu S, Strowig T, Eynon EE, Frleta D, Gurer C, Murphy AJ, Yancopoulos GD, et al. A novel humanized mouse model with significant improvement of class-switched, antigen-specific antibody production. Blood. 2017;129:959–969. [PubMed: 28077418]

Author Manuscript Author Manuscript Author Manuscript Author Manuscript

Clinical Perspective

What is new?

- We describe a new cellular mechanism linking ischemia reperfusion injury to the development of donor specific antibody, a pathologic feature of chronic antibody-mediated rejection mediating late graft loss.

What are the clinical implications?

- Therapies targeted against endothelial cell-derived factors like IL-18 may block late complication of ischemia reperfusion injury

Author Manuscript Author Manuscript Author Manuscript Author Manuscript

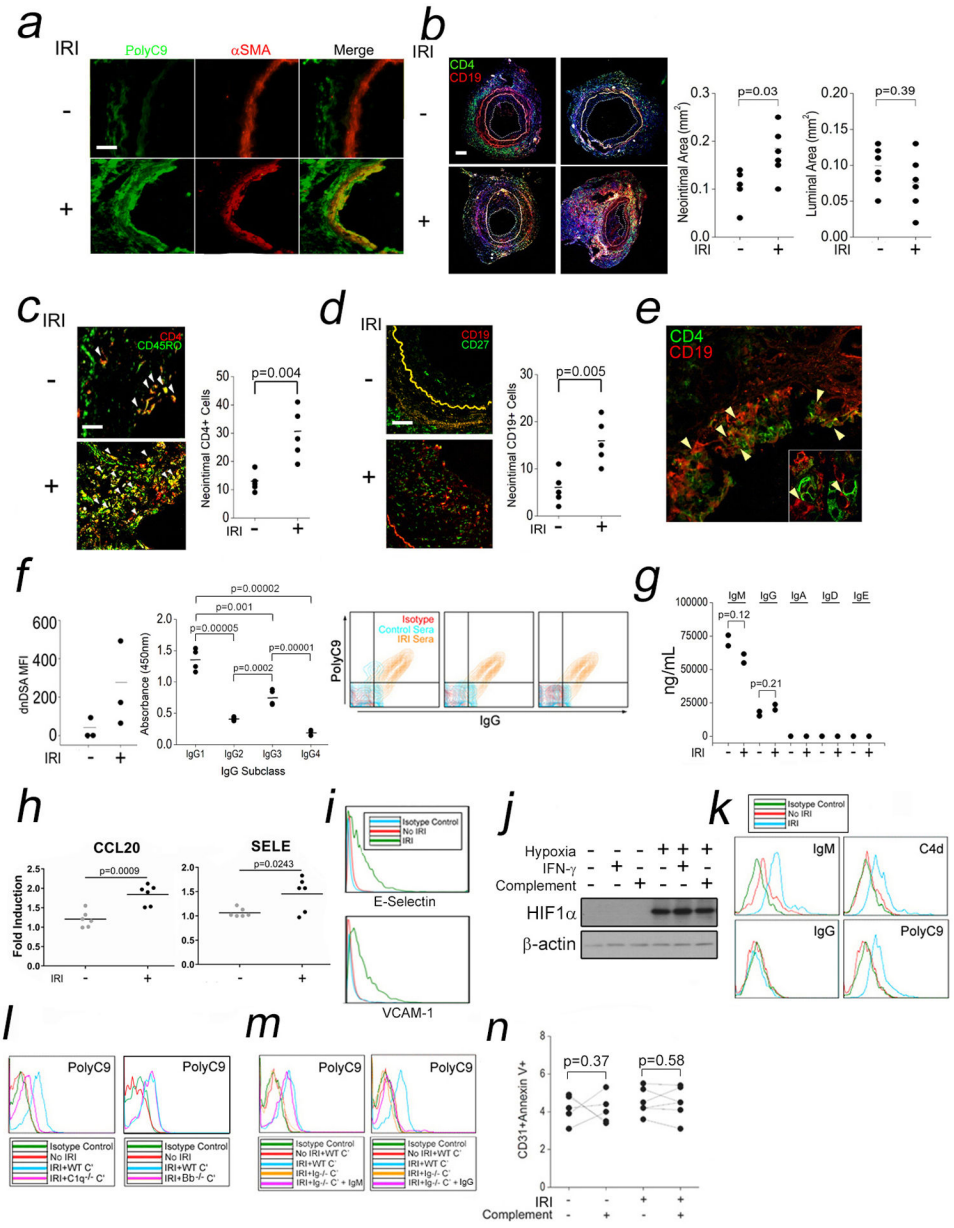

Fig 1. Humanized Models of IRI to Recapitulate Features of CABMR.

Human coronary artery grafts were subjected to *ex vivo* normoxia or hypoxia for 12h prior to implantation as infrarenal interposition grafts in descending aortae of SCID/bg mice engrafted with human lymphoid cells. Four weeks after implantation, artery tissues were harvested for analysis. Control (n=6) and IRI-treated (n=6) xenografts were analyzed for MAC (PolyC9, *a*, scale bar: 200μm), vasculopathy (*b*, scale bar: 400μm), neointimal CD4+CD45RO+ T cells (*c*, scale bar: 200μm), CD19+CD27+ B cells (*d*, scale bar: 200μm), and CD4+ T cell:CD19+ B cell "conjugates" (*e*). Total dnDSA (*f*, left) and dnDSA IgG subclasses from host sera were quantified (*f*, middle). HUVEC were pretreated with IFN-γ (50ng/mL) for 48h prior to overlay of control or murine sera (25% v/v) in gelatin veronal buffer for 2h prior to FACS analysis (*f*, right). Sera Ig isotypes were quantified (*g*). HUVEC subjected to "IRI" were analyzed by qRT-PCR (*h*), FACS (*i*), and Western blot (*j*). Cells

Author Manuscript Author Manuscript Author Manuscript Author Manuscript

were analyzed by FACS after "IRI" (*k*) and in the presence of WT, C1q, (*l*, left) or Bb-deficient (*l*, right) human sera. HUVEC were subjected to "IRI" using total Ig-depleted sera in the presence of exogenous IgM (2mg/mL) or IgG (8mg/mL) and analyzed by FACS (*m*). HUVEC were subjected to "IRI" and assessed by FACS (*n*). Student's *t*-test was used for Fig 1*b*, 1*c*, 1*d*, 1*f*, left, 1*g*, and 1*h*. One-way ANOVA followed by Tukey's pairwise comparison was used for Fig 1*f*, middle. A two-way repeated measured ANOVA was used for Fig 1*n*. Experiments above were repeated 2–6 times using ≥2 pools of HUVEC donors.

Author Manuscript Author Manuscript Author Manuscript Author Manuscript

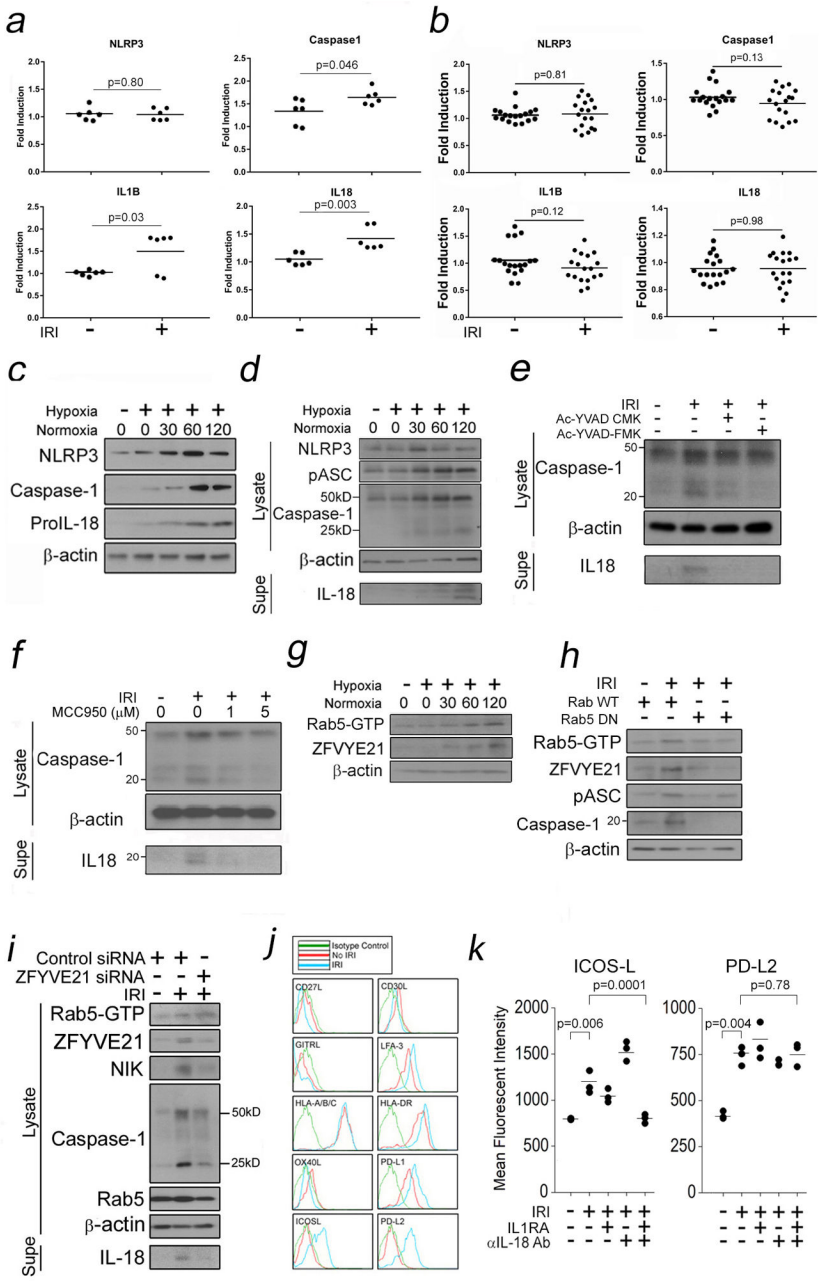

Fig 2. A Rab5-ZFYVE21-NIK Axis Activates an NLRP3 Inflammasome in "IRI"-Treated EC.

Following "IRI" without (a) or with IFN-γ pretreatment (*b*, 50ng/mL for 48–72h), HUVEC were tested by qRT-PCR. Western blots of HUVEC lysates after 4h of hypoxia followed by varying normoxia times (*c*). Western blots of "IRI"-treated HUVEC subjected to 4h of hypoxia followed by 2h of normoxia (*d*). HUVEC were pretreated for 30min with Ac-YVAD-CMK or Ac-YVAD-FMK prior to "IRI" (*e*). HUVEC were pretreated with MCC950 as indicated for 30min prior to "IRI" (*f*). "IRI"-treated HUVEC were assessed by Western blot (*g*). HUVEC stably transduced with Rab5 WT or Rab5 DN constructs were probed by Western blot following "IRI" (*h*). Western blot analysis of EC transfected with control or ZFYVE21 siRNA (*i*). "IRI"-treated HUVEC were analyzed by FACS (*j*) in the presence or

Author Manuscript Author Manuscript Author Manuscript Author Manuscript

absence of depleting Ab as indicated (*k*). Student's *t*-test was used for Fig 2*a* and 2*b*. One-way ANOVA followed by Tukey's pairwise comparison was used for Fig 2*k*. Experiments were repeated 2–4 times using ≥2 HUVEC donors.

Author Manuscript Author Manuscript Author Manuscript Author Manuscript

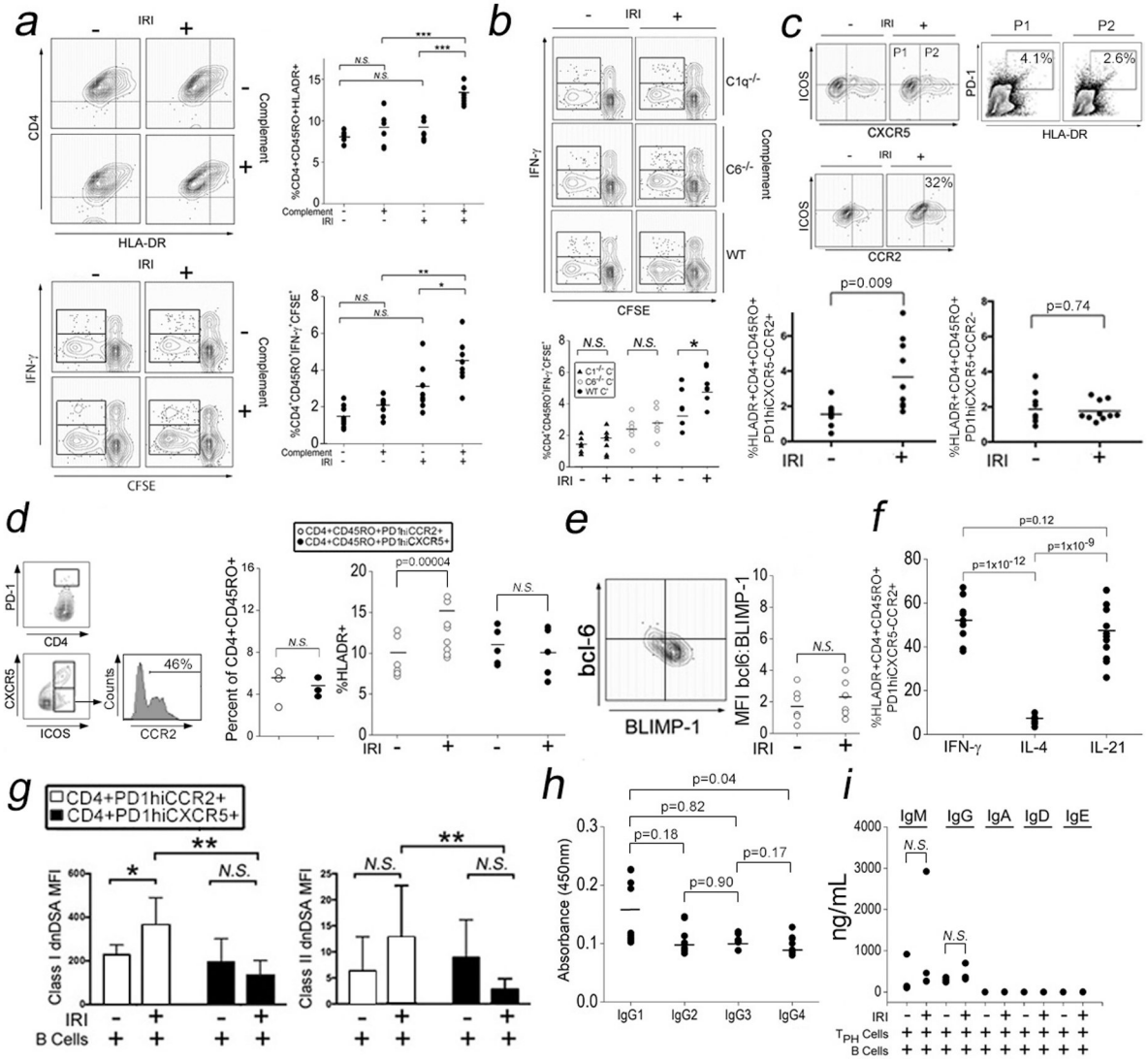

Fig 3. "IRI"-Treated EC Selectively Expand T_{PH} Cells *In Vitro*.

HUVEC were subjected to "IRI" in the presence or absence of normal human sera as a source of complement (C') prior to co-culture with CD4+CD45RO+ T cells (T_{mem}) for 7–10 days prior to T cell analysis for activation (*a*, top) and proliferation (*a*, bottom). ***p<0.001, **p<0.005, *p<0.05, *N.S.* not significant (p>0.05). T_{mem} cocultured with HUVEC subjected to "IRI" in the presence of WT C', C1q-deficient C', or C6-deficient C' (*b*). T_{mem} were cocultured with IRI-treated EC and analyzed for CD4+CD45RO+PD-1+CXCR5-CCR2+ and CD4+CD45RO+PD-1+CXCR5+CCR2- T cells (*c*). FACS-sorted T cells were cocultured with IRI-treated EC as indicated and analyzed by FACS (*d*). T_{mem} were cocultured with EC for 7–10 days and bcl-6:BLIMP ratios were assessed (*e*). T_{mem} were cocultured with EC for 14 days and intracellular cytokines were analyzed (*f*). "IRI"-treated EC were cocultured with FACS-sorted T cells in the presence of autologous B cells for 14 days, and supernatant titers of anti-class I (*g*, left) and anti-class II (*g*, right) HLA Ab specific for cultured EC, i.e., dnDSA, were quantified (*g*) along with dnDSA IgG subclasses (*h*). Total Ig isotypes were quantified by ELISA (*i*). Student's *t*-test was used for Fig 3*c*.

Author Manuscript Author Manuscript Author Manuscript Author Manuscript

One-way ANOVA followed by Tukey's pairwise comparison was used for Fig 3*g*, 3*h*, and 3*i*. Two-way ANOVA followed by Tukey's pairwise comparison was used for Fig 3*a*, 3*b*, 3*d*, and 3*f*. Experiments were repeated 2–8 times using ≥2 PBMC donors and ≥2 HUVEC donors.

Author Manuscript Author Manuscript Author Manuscript Author Manuscript

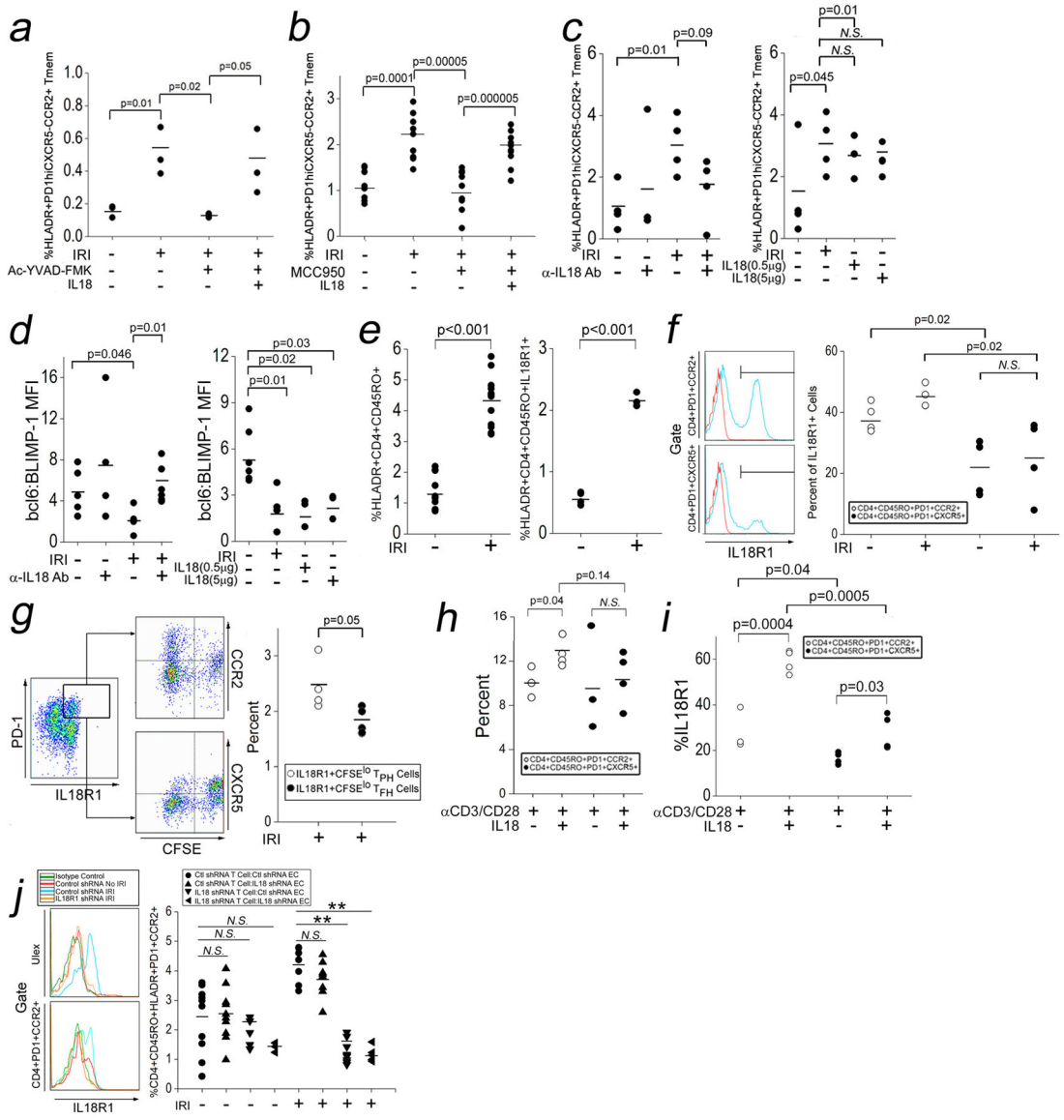

Fig 4. IL-18 Directly Expands IL-18R1+ T_{PH} Cells.

EC were treated with Ac-YVAD-FMK (*a*) or MCC950 (*b*) during "IRI" prior to coculture with CD4+CD45RO+ T cells (T_{mem}) in the presence or absence of exogenous IL-18 (0.5μg) as indicated for 10 days prior to FACS analysis. T_{PH} cells and T_{FH} cells were gated among T_{mem} cocultured with "IRI"-treated ECs in the presence IL-18-depleting antibody (10μg/mL, c, *left*) or exogenous IL-18 as indicated (c, *right*). Mean fluorescent intensities (MFI) of bcl-6 and BLIMP1 were assessed in T_{mem} with αIL-18 Ab (*d*, left) or exogenous IL-18 (*d*, right) following coculture with IRI-treated EC. T_{mem} were stimulated with "IRI"-treated EC (*e*). IL-18R1 expression after gating on T_{PH} and T_{FH} cell populations following 7 day coculture with "IRI"-treated HUVEC (*f*). T_{PH} and T_{FH} cells were analyzed after gating on IL-18R1 (*g*). T_{mem} were stimulated with αCD3/CD28 for 24h prior in the presence or absence of IL-18 (*h,i*). IL-18R1 shRNA was transduced into "IRI"-treated HUVEC, T_{mem}, or both prior to EC:T cell coculture for 7 days (*j*, **p<0.001, *N.S.*, not significant).

Author Manuscript Author Manuscript Author Manuscript Author Manuscript

Student's *t*-test was used for Fig 4*e* and 4*g*. Two-way ANOVA followed by Tukey's pairwise comparison was used for Fig 4*a*, 4*b*, 4*c*, 4*d*, 4*f*, 4*h*, 4*i*, and 4*j*. Experiments were repeated 2–6 times using ≥3 PBMC donors and ≥2 HUVEC donors.

Author Manuscript Author Manuscript Author Manuscript Author Manuscript

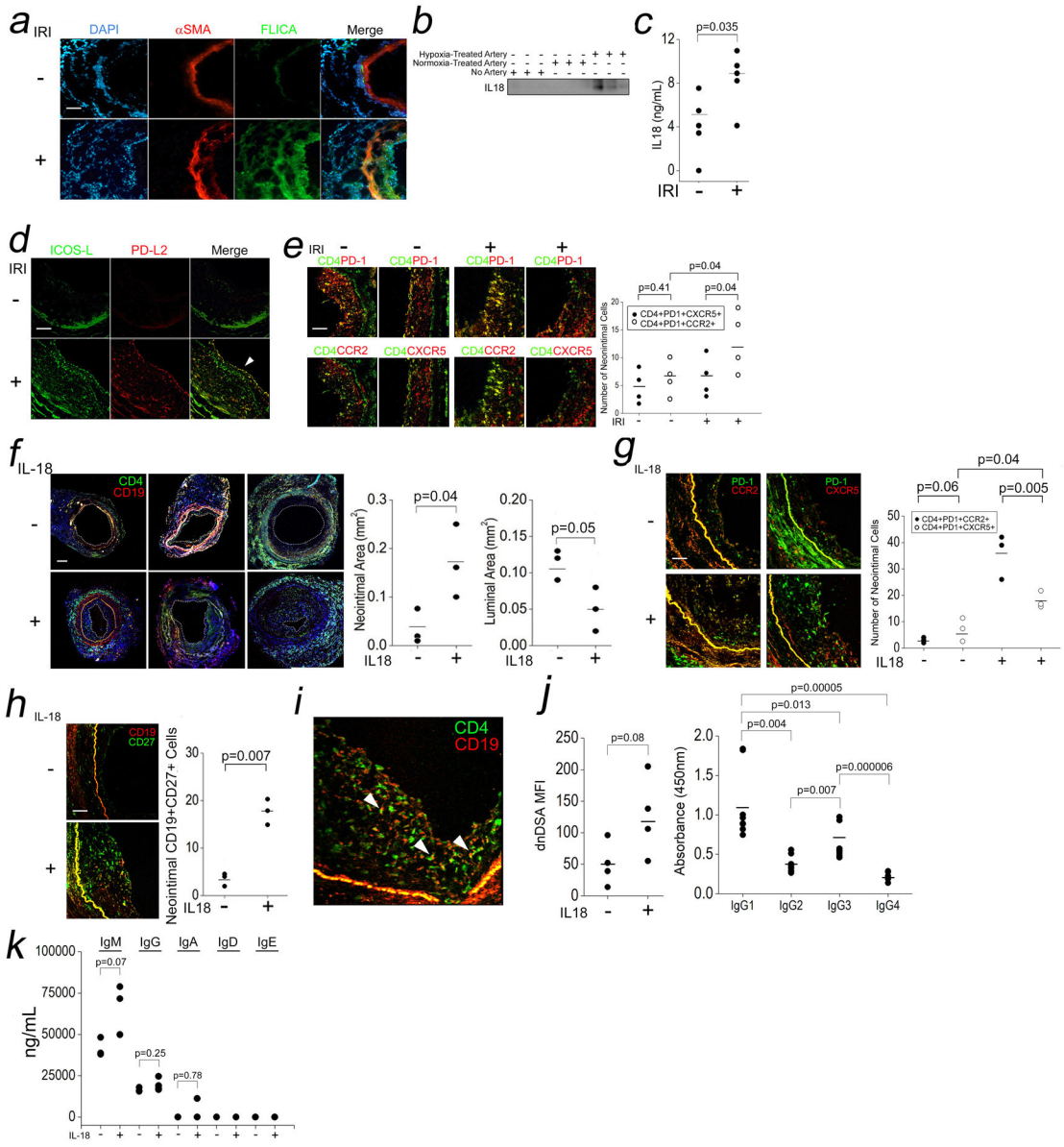

Fig 5. IRI-Induced Inflammasomes in EC and IL-18-Mediated T_{PH} Cell Expansion *In Vivo*.

Human coronary artery grafts were subjected to *ex vivo* hypoxia and surgically implanted into descending aortae of SCID/bg mice for 24h prior to analysis by I.F. for FLICA (*a*, scale bar: 200μm) and sera were analyzed by Western blot IL-18 (*b*) and ELISA (*c*). n=3–5 for the above experiments. Grafts were analyzed for ICOS-L and PD-L2 (*d*, 250μm) and T_{PH} and T_{FH} cell infiltrates (*e*, scale bar: 250μm). Hosts bearing normoxia-treated human arteries were injected *i.p.* with vehicle or IL-18 (10μg/dy) for 14 days. Neointimal and luminal areas were calculated (*f*, scale bar: 400μm), and neointimal T_{PH} cells and T_{FH} cells were quantified (*g*, scale bar: 250μm) along with CD19+CD27+ B cells (*h*). CD4+:CD19+ cell "conjugates" were visualized in neointimal tissues (*i*). Sera was tested for dnDSA Ab titers (*j*, left), dnDSA IgG subclasses (*j*, right), and Ig isotypes (*k*). Student's *t*-test was used for Fig 5*c*, 5*f*, 5*h*, and 5*j*, left. One-way ANOVA followed by Tukey's pairwise comparison was

Author Manuscript Author Manuscript Author Manuscript Author Manuscript

used for Fig 5*j*, right, *and* 5*k*. Two-way ANOVA followed by Tukey's pairwise comparison was used for Fig 5*e* and 5*g*.

Author Manuscript Author Manuscript Author Manuscript Author Manuscript

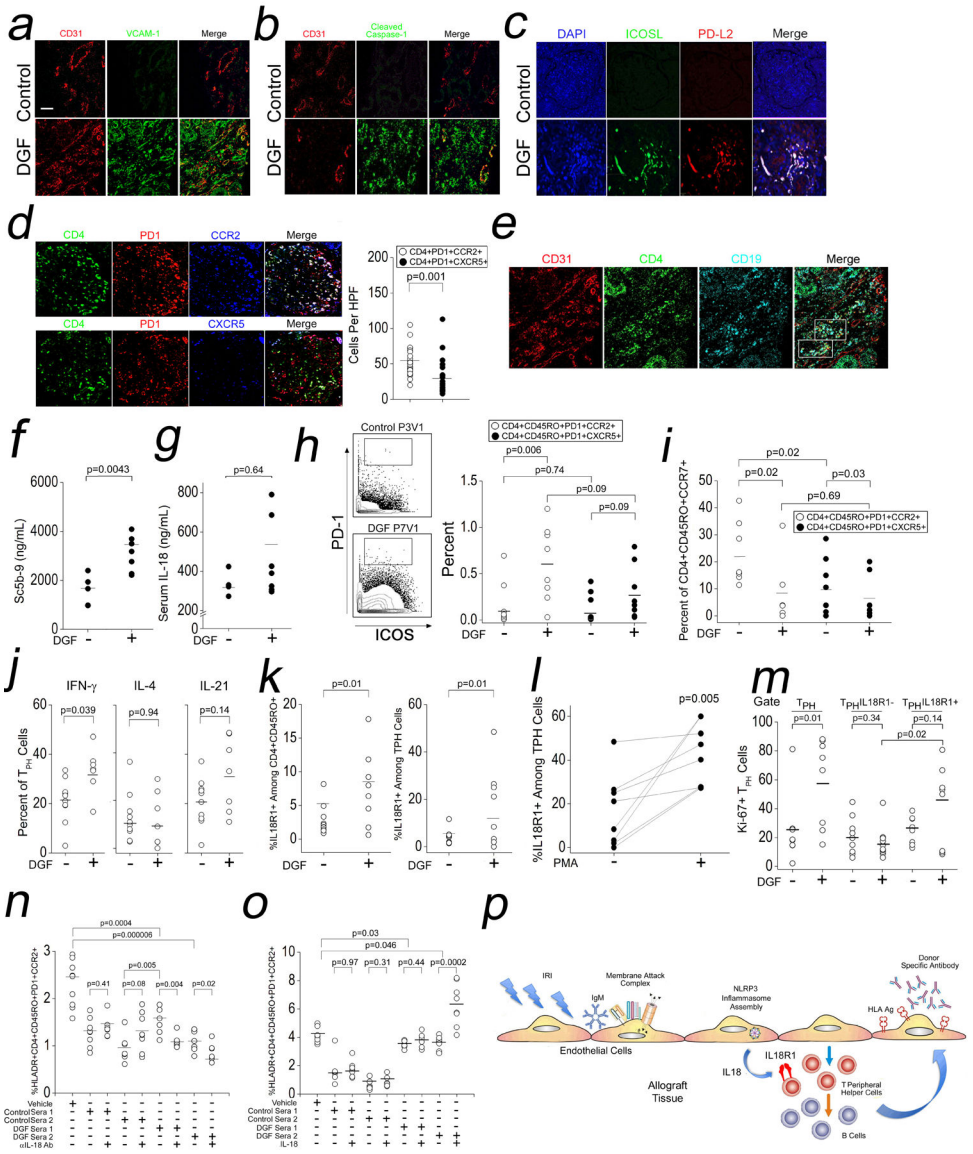

Fig 6. IL-18-Dependent Expansion of IL-18R1+ T_{PH} Cells in DGF Patients.

Archived biopsies from patients with DGF who developed CABMR were analyzed by I.F. (*a-e*). Prospectively collected sera from control or DGF renal transplant patients were assessed for complement activation (*f*) and IL-18 (*g*). PBMCs from control or DGF renal transplant patients were analyzed by CyTOF (*h-m*). In (*j*) and (*l*), PBMCs were stimulated for 4h with PMA/ionomycin prior to CyTOF analysis. Non-autologous T_{mem} were stimulated with αCD3/CD28 for 24hr in the presence of 10% v/v autologous sera from DGF or control patients in the presence αIL-18 Ab (*n*) or exogenous IL-18 (*o*). Proposed model connecting IRI with CABMR (*p*). Scale bars: 300μm. Student's *t*-test was used for Fig 6*d*, 6*f*, 6*g*, 6*j*, 6*k*, and 6*l*. Two-way ANOVA followed by Tukey's pairwise comparison was used for Fig 6*h*, 6*i*, 6*m*, 6*n*, and 6*o*.

Author Manuscript
Author Manuscript
Author Manuscript
Author Manuscript

Table 1.

Baseline Characteristics of Control and DGF Patients.

Patient Characteristic	Control (n=10)	DGF (n=8)	p-value
Age (Mean±SD)	47.2±12.1	48.13±11.4	0.68
Gender (%Male/%Female)	40/60	50/50	0.79
Body Mass Index (BMI)	30.89±6.16	31.65±3.32	0.21
Hospitalization Length (Days, ±SD)	4.2±0.45	7.0±2.44	0.04
Creatinine (±SD)	1.51±0.67	2.498±1.29	0.11
Calculated Panel Reactive Antibody (PRA, %, ±SD)	17.2±37.2	41.13±41.4	0.003